

Copyright © 2003 by the author(s). Published here under licence by The Resilience Alliance.

The following is the established format for referencing this article:

Wade, T. G., K. H. Riitters, J. D. Wickham, and K. B. Jones. 2003. Distribution and causes of global forest fragmentation. *Conservation Ecology* 7(2): 7. [online] URL: <http://www.consecol.org/vol7/iss2/art7>

Report

Distribution and Causes of Global Forest Fragmentation

[Timothy G. Wade](#)¹, [Kurt H. Riitters](#)², [James D. Wickham](#)¹, and [K. Bruce Jones](#)¹

¹*U.S. Environmental Protection Agency, National Exposure Research Laboratory*, ²*U.S. Forest Service*

- [Abstract](#)
 - [Introduction](#)
 - [Methods](#)
 - [Results](#)
 - [Discussion](#)
 - [Acknowledgments](#)
 - [Responses to this Article](#)
 - [Literature Cited](#)
-

ABSTRACT

Because human land uses tend to expand over time, forests that share a high proportion of their borders with anthropogenic uses are at higher risk of further degradation than forests that share a high proportion of their borders with non-forest, natural land cover (e.g., wetland). Using 1-km advanced very high resolution radiometer (AVHRR) satellite-based land cover, we present a method to separate forest fragmentation into natural and anthropogenic components, and report results for all inhabited continents summarized by World Wildlife Fund biomes. Globally, over half of the temperate broadleaf and mixed forest biome and nearly one quarter of the tropical rainforest biome have been fragmented or removed by humans, as opposed to only 4% of the boreal forest. Overall, Europe had the most human-caused fragmentation and South America the least. This method may allow for improved risk assessments and better targeting for protection and remediation by identifying areas with high amounts of human-caused fragmentation.

KEY WORDS: forest fragmentation, forest pattern, global, risk assessment, targeting.

Published: September 4, 2003

INTRODUCTION

Global deforestation has been documented extensively, with an emphasis on the loss of tropical rainforests in Central Africa and Amazonia and the impacts on global climate and carbon budgets (Fearnside 1996, Laurance 2000, Justice et al. 2001, Semazzi and Yi 2001, Zhang et al. 2001). Another consequence is change in forest dynamics from fragmentation. Alteration of forest spatial patterns affects wildlife habitat quality and biodiversity in both tropical forests (Gascon and Lovejoy 1998, Carvalho and Vasconcelos 1999, Scariot 1999, Laurance et al. 2000) and extra-tropical forests (Jules et al. 1999, Hargis et al. 1999, Kurki et al. 2000, Virgos 2001).

Forest area statistics are available from several sources. The United Nations Food and Agriculture Organization (FAO) produces the *Forest Resources Assessment* every 10 years, which estimates global forest area and change over time (Holmgren 2001), and the World Resources Institute (WRI) has published the *Pilot Analysis of Global Ecosystems*, which includes a forest ecosystems component (Matthews et al. 2000). Estimates for some areas are based on incomplete or inconsistent data, and methodological differences make comparisons difficult (Matthews 2001). Nevertheless, in the preceding decade we have witnessed a continuing reduction in global forest area with apparently substantial reductions occurring mainly in tropical areas.

There has not been a systematic analysis of human vs. natural sources of forest fragmentation at the global scale. Frontier forests, defined as “large, ecologically intact, and relatively undisturbed natural forest,” have been mapped globally and a qualitative threat rating has been assigned to each patch (Bryant et al. 1997). Pahari and Murai (1999) demonstrated the high correlation between human population density and cumulative forest loss for regions. Matthews et al. (2000) recognized fragmentation as an issue separate from forest loss, and discussed deforestation and fragmentation caused by humans on a global scale. Riitters et al. (2000) quantified total forest fragmentation across multiple evaluation scales but did not identify human-caused fragmentation. Jones et al. (1999) assessed forest patch vulnerability based on edge shared with anthropogenic and natural land uses but only examined three tropical areas. A systematic global assessment is needed because anthropogenic land uses tend to expand or change over time and, as a result, areas that now experience human-induced fragmentation are more likely to be areas of changing forest patterns in the future. This is especially true in tropical regions experiencing direct forest loss, but also applies to shifts in land uses in regions where total forest area is more or less constant, such as in North America.

Forests may be fragmented by a number of activities or events, such as road construction, logging, conversion to agriculture, or wildfire, but ultimately, the fragmenting cause is either anthropogenic or natural in origin. In this paper, we present a method to calculate the amount of human and naturally caused forest fragmentation on a global scale using 1-km land cover data. The method quantifies fragmentation based on edges between forest and neighboring pixels, and identifies the cause as either anthropogenic or natural. We report the amount of anthropogenic and natural forest fragmentation for six continents by World Wildlife Fund (WWF) biomes (Olson et al. 2001). Because of interest in tropical forest ecosystems, we also report the results by WWF ecoregions for the tropical and subtropical moist broadleaf forest biome (TrMB hereafter) in South America.

METHODS

We used land cover maps from the Global Land Cover Characteristics (GLCC) database (version 2.0). The maps were derived from advanced very high resolution radiometer (AVHRR) satellite imagery acquired between April 1992 and March 1993 and have a spatial resolution of 1 km (Loveland et al. 2000). The GLCC distributes maps of Eurasia as a single entity; we separated this into Europe (including the Arabian Peninsula) and Asia along an axis tracing the Ural Mountain Range. We used the 17-class International Geosphere Biosphere Programme (IGBP) map legend (Loveland and Belward 1997) and re-classified each pixel as anthropogenic, forest, or other natural land cover types (Table 1). Snow, ice, and water bodies were treated as missing data and were not permitted to fragment the forest land cover in the analysis.

For data summaries, we used selected WWF biomes (Olson et al. 2001) to stratify the continental analyses of fragmentation (Fig. 1A–F). Eight forest and woodland biomes were considered; forest land in other biome types was not included in our analysis. To facilitate later comparisons, we also calculated the percentage of each global biome found on each continent (Table 2) and the percentage of the global biome area that was in each of the three land cover types on each continent (Table 3).

To perform the fragmentation calculations, we used a “moving window” algorithm (e.g., Riitters et al. 2000) with a single window size of 9×9 pixels (i.e., 8100 ha). The window was centered on each land cover pixel (forested or not), a fragmentation score was calculated for the window, and the result was assigned to the center pixel. Maps of four indices were produced for each continent to characterize forest fragmentation by anthropogenic pixels (P_{fa}), forest fragmentation by non-forest natural land cover pixels (P_{fn}), overall forest connectivity (P_{ff}), and forest area density (P_f). The computations are illustrated in Fig. 2. Using the same algorithm as Riitters et al. (2000), P_f was the proportion of the window that was forest, and P_{ff} was the ratio of the number of adjacent (cardinal directions only) pixel pairs for which both pixels were forest to the number of adjacent pixel pairs where either one or both pixels was forest.

A new method was developed to partition total forest fragmentation into components that correspond to P_{fn} and P_{fa} sources. First, we defined total fragmentation (F_t) as the sum of natural and anthropogenic fragmentation, and the complement of overall forest connectivity:

$$F_t = (P_{fn} + P_{fa}) = (1 - P_{ff})$$

To compute the natural component of total forest fragmentation (P_{fn}), we used the same denominator as for P_{ff} , and calculated the proportion of adjacent pixel pairs involving forest for which one pixel was forest and the other was a non-forest, natural land cover type. Similarly, fragmentation due to humans (P_{fa}) was the proportion of adjacent pixel pairs involving forest for which one pixel was forest and the other was an anthropogenic land use type. All of the indices range from 0 to 1 and were rescaled to a range of 0 to 100 for data summaries.

Some forest biomes contain relatively little forest and, as a result, indices based on the present

forest will underestimate fragmentation owing to deforestation. The following procedure was used in an attempt to capture that aspect of fragmentation. Windows containing no forest, whose center cell had an anthropogenic land use, were assigned P_{fa} values of 100 (and P_{fn} and P_{ff} were set to zero). The rationale is that, because only forest biomes were considered, any location that was developed and whose surrounding 9×9 neighborhood contained no forest, was more likely to have been deforested than to have never supported forest at all. Our rationale is supported by the observation that globally, 70% of the windows that met the conditions were >95% developed. Note that P_{fa} also equals 100 if a window contains only isolated forest pixels that are only adjacent to developed pixels, and our procedures do not distinguish between the two cases. The procedure may overestimate anthropogenic fragmentation in biomes with large proportions of non-forest natural land cover (e.g., temperate coniferous in Asia and Europe, boreal in North America, and Mediterranean on all continents; see Table 2). Conversely, when land cover was non-forest natural and the associated neighborhood contained no forest, the cell was ignored in analyses. This case assumes that the area was a non-forested patch within the forest biome that never supported forest. Under these assumptions, P_{fa} reflects both the amount of forest and its fragmentation relative to undisturbed conditions.

Several tabular and graphical summaries were generated to assist in the interpretations of the relationships between P_{ff} , P_{fa} , P_{fn} , and P_f . Tabular summaries were prepared for eight forest biomes and six continents, but only 36 of the possible 48 combinations were realized because some biomes did not occur on some continents. The forest connectivity index (P_{ff}) was also summarized based on threshold values of 60% ("connected") and 100% ("interior"), where the 60% threshold was chosen by analogy to percolation theory (Stauffer 1985), assuming a random distribution of forest in a window (Gardner et al. 1987). Tables were prepared to show average P_{fa} and P_{fn} values by percentage for forest WWF biomes by continent and, for the one biome in South America, by using WWF ecoregions within that biome. A scatter plot of average biome P_f and P_{fa} by continent was also produced to allow graphical interpretation of the data.

After Milne (1992), color composites of P_{ff} (green), P_{fa} (red), and P_{fn} (blue) were constructed to provide spatial views of the changing dominance of the individual metrics in different places. To saturate color and improve legibility, the highest value among P_{ff} , P_{fa} and P_{fn} was multiplied by a scaling factor so that it equaled 255. Each of the other two values was also multiplied by the same factor. The color composite maps show highly connected forest in green, and forest with large amounts of natural fragmentation in blue. Deforested areas and forest that was highly fragmented by human use are shown in red. Areas where P_{ff} and P_{fa} were approximately equal are rendered in yellow and areas where P_{ff} and P_{fn} were approximately equal are displayed in cyan. Pixels that were a non-forest natural class and had no forest in their 9×9 window were displayed in black, and missing values (including non-forest biomes) were shown in white.

The color composite maps were complemented by maps illustrating the standard deviation of P_{fa} . Although the composite maps display absolute amounts of P_{ff} , P_{fa} and P_{fn} , standard deviation maps show the level of P_{fa} relative to the rest of the biome by continent. These maps were constructed by first calculating the mean and standard deviation P_{fa} value for each

continent and biome. Any pixel with a P_{fa} value more than two standard deviations above the mean was then displayed in red, pixels between one and two standard deviations above the mean were pink, and pixels within one standard deviation of the mean were white. Pixels between one and two standard deviations below the mean were shown in light green, and pixels more than two standard deviations below the mean were dark green. In many biomes, the standard deviation was greater than the mean and, as a result, it was impossible to have any green areas in the biome. To compensate for that artifact, the areas with no fragmentation (P_{fa} values of zero) were always displayed in dark green.

RESULTS

The continental proportion of forest in a biome that is “connected” (i.e., $P_{ff} \geq 60\%$) is a general indicator of the degree of fragmentation, and the proportion that is “interior” ($P_{ff} = 100\%$) indicates how much forest is relatively remote from other land cover types. At least half the biome area was “connected” forest in 18 of the 36 combinations of biome and continent (Table 4), and 11 of the 18 cases were in North and South America. Only one of six biomes in Africa, and one of four in Europe were more than half “connected” forest. In all these cases, forest tends to be the dominant land cover type in the locations where forest is found. Relatively high proportions of “interior” forest were found in the TrMB biome in Africa and South America, and in all boreal biomes.

Table 5 shows the partitioning of fragmentation into anthropogenic and natural components. Globally, with the exception of the boreal and temperate conifer forest biomes, human-caused fragmentation was typically at least three times more prevalent than natural fragmentation. Out of 36 combinations of biome and continent, anthropogenic fragmentation was greater than natural fragmentation in 27 cases. In the TrMB and temperate broadleaf and mixed forest biomes, which together account for over half of all forest cover, P_{fa} was substantially higher than P_{fn} . Europe was particularly impacted by human fragmentation in all forest biomes. Even in the boreal forest biome, which globally had low fragmentation and little human influence, P_{fa} was almost three times greater than P_{fn} , indicating that most fragmentation was anthropogenic in origin. This is not entirely unexpected, as we only used forest biomes where conversion was more likely to be a result of human activity than natural forces, increasing P_{fa} relative to P_{fn} . Of the nine cases where natural fragmentation was greater than human fragmentation, eight occurred in biomes that occupied less than 2% of the continental area (e.g., mangroves) or that could be considered as “naturally patchy” biome types (e.g., Mediterranean or boreal). Africa was affected more by natural fragmentation in four of six biomes, but the area contained in three of these biomes was very small.

It is helpful to evaluate human-caused fragmentation by taking into account the amount of forest that is represented (Fig. 3). Biomes with a high (or low) proportion of forest are necessarily less (or more) fragmented according to our model. However, for a given amount of forest, there can be more or less human-caused fragmentation depending on the biome, and the differences among biomes may indicate opportunities for restoration or preservation. Except for boreal forests, European forests were in the poorest condition, with very low P_f and

very high P_{fa} . South American forests were in the best condition, with high P_f and low P_{fa} relative to the other continents, especially in the TrMB biome, which contained most of the forest on the continent. Because of the high level of current interest in tropical forest condition in general and Amazonia in particular, fragmentation was further stratified by ecoregion for the TrMB biome in South America. Average P_{fa} and P_{fn} for the biome were 13.43 and 4.21, respectively, but the 54 component ecoregions ranged from 2.02 to 86.75 for P_{fa} and 0.05 to 36.30 for P_{fn} (Table 6).

Color composite maps (Fig. 4A–F) show specific areas representing human-caused (red) and natural (blue) forest fragmentation and well-connected forest (green). Yellow delineates transitions between areas of high connectivity and high human fragmentation and cyan identifies ecotones. As only forest biomes were included, ecotones were somewhat uncommon on the maps. The maps clearly showed the areas dominated by anthropogenic fragmentation and generally low amount of P_{fn} globally. In particular, the non-boreal forest biomes in Asia (Fig. 4B) and Europe (Fig. 4D) showed widespread human fragmentation. The TrMB biome in Africa (Fig. 4A) and South America (Fig. 4F) were largely intact except in coastal regions. Natural fragmentation was found most commonly in Asia (Fig. 4B) and North America (Fig. 4E) where boreal forest gave way to tundra.

Standard deviation maps (Fig. 5A–F) compared P_{fa} values within biomes for each continent. Patterns in these maps had much in common with the color composites, as areas of high absolute P_{fa} also had generally high P_{fa} relative to the rest of the biome. Perhaps most interesting was Europe (Fig. 5D), which had extremely high P_{fa} values relative to other continents and was mostly red in Fig. 4D. By using relative P_{fa} values within Europe, forests appeared to be in good condition (Fig. 5D) with patches of below average P_{fa} (light green) scattered throughout the continent. The only red area was the southern edge of the boreal forest, with the largest patch located in northwest Russia.

DISCUSSION

Summaries of forest connectivity by biome and continent were useful as an indicator of general condition. Comparing biome values across continents provided insight into global variation. Almost 50% of South American TrMB was interior forest, compared with only 16% in Asia. These summaries did not provide information on causes of low connectivity (high fragmentation).

Similar to connectivity summaries, summarizing P_{fa} and P_{fn} using biomes was useful as a broad indicator of forest fragmentation. Information about relative condition was again available by comparing across continents, but causes behind the fragmentation can now be quantified. The value of separating P_{fa} from overall fragmentation for targeting purposes was evident in naturally patchy forest biomes. Total fragmentation in the boreal forest of North America was almost 23%, but practically all was due to natural fragmentation. Because of the low level of human-caused fragmentation, protection or remediation measures are not likely to be necessary.

Biomes, however, were too large for summaries of P_{fa} and P_{fn} to be effective targeting tools for specific at-risk areas. For example, the TrMB biome in South America covered nearly half the continent, and the low overall P_{fa} masked local problem areas, such as Rondonia where widespread deforestation has occurred. Smaller reporting units can provide more useful targeting information. Summaries using 54 WWF ecoregions in the TrMB biome in South America reveal that all 27 ecoregions with P_{fa} over 20% were coastal or near-coastal. However, the Madeira-Tapajós moist forests ecoregion, which contains the Rondonia area, still had a low P_{fa} of 4.79. The optimal way of targeting specific areas is to use P_{fa} values at the pixel level.

Composite maps (Fig. 4A–F) are a useful way to identify local hot spots, by using actual P_{fa} , P_{fn} , and P_{ff} pixel values instead of averages for a summary area. In South America, development in the Rondonia region was clearly visible in the Amazon basin as a large area of red and yellow patches (Fig. 4). Globally, areas displayed in yellow represented transition zones between connected forest and human-fragmented forest. With continued, contagious human land-use expansion, these areas will be the most likely to experience further degradation. In time, the transition zones may become highly fragmented and new transitional areas will appear deeper in the intact forest. Consequently, the yellow areas on the composite maps may represent excellent opportunities for protection or restoration. Protecting transitional and adjacent areas may limit further expansion or degradation of the transitional areas. Restoration efforts to eliminate or reduce fragmentation may produce larger patches of connected or interior forest. This is particularly true in the TrMB biome in South America, currently the least fragmented of the major forests. There are numerous small patches of transitional areas that, if allowed to expand, could result in significant forest fragmentation and removal.

Standard deviation maps (Fig. 5A–F) are similar to composite maps in that they are useful for identifying specific areas of concern. Mapping relative human-caused fragmentation may be more useful for policy makers than composite maps. In Europe, for example, where temperate forests have largely been removed, the standard deviation map identified small patches with less or even no fragmentation. These areas could be prioritized for protection. Conversely, in South America, where the TrMB biome was mostly intact, areas with average or higher amounts of fragmentation might be good candidates for restoration.

One goal of decision makers might be to maximize forest connectivity (Wickham et al. 1999). Critical values of P_f are 40 and 60% according to percolation theory (Stauffer 1985). Figure 3 could be used as a general targeting tool to locate biomes near critical levels. Where P_f is at or above 60%, protective measures might be taken. Where P_f is between 40 and 60%, restoration might be undertaken, using composite maps, standard deviation maps, or some other tool to identify specific areas where actions would have the greatest impact. In addition, biomes with smaller amounts of forest are likely at higher risk than biomes with larger amounts of forest given equal P_{fa} values. Figure 3 could help identify these areas. As an example, the P_{fa} values were fairly low in the temperate conifer forest biome for both Asia (13.3%) and North America (11.6%). However, the P_f value was much higher in North America (75–49%), which places Asian temperate conifer forests at higher risk.

At 1-km resolution, the GLCC data represents generalized land cover. Consequently, only very large urban areas are identified and the majority of anthropogenic-caused fragmentation at this scale was due to agriculture. The smoothing effect of coarse-resolution data overemphasized the dominant land cover. In forested areas, it produced a “best case” fragmentation picture. Roads, a very important fragmenting agent (Riitters and Wickham 2003), and small perforations in the forest were not detected, creating a much more connected map than exists in reality. In human-dominated landscapes, forest may be portrayed as completely absent, when, in fact, small forest patches may exist.

The GLCC data is now over 10 years old, so recent development is not represented in our analyses. One example of underestimating fragmentation due to spatial and temporal limitations of the land cover was in the Amazonia region of South America. Although large areas of contiguous forest still exist, government policies have encouraged development in recent decades, including the construction of major highways (Laurance 2000). More recent, higher resolution land cover would better detect major roads and new urban and agricultural development, drastically increasing anthropogenic fragmentation scores in parts of the region.

A recent global land cover database derived from the MODIS sensor on the Terra satellite is currently under development (Friedl et al. 2002). An initial dataset is available, but substantial differences between the MODIS and GLCC precluded comparisons in this study. The MODIS land cover is expected to be updated quarterly, and should be valuable for identifying fragmentation trends in the future.

Non-forest biomes were not included in this study. The assumption that windows containing no forest, with an anthropogenic land use in the center pixel, were deforested would have been incorrect in these biomes. Clearly, forests in these regions could be important. A simple modification to the model could alter the assumption to ignore those pixels instead of classifying them as deforested. In this case, the assumption would be that windows with no forest never contained forest and would be displayed in white on a composite map regardless of center pixel land cover.

Forest fragmentation disregards threats to other important natural land cover types, such as wetlands, grasslands, and shrublands. The method presented in this paper can be easily extended to calculate fragmentation of any land cover type. The method presented is scale independent. Raster land cover data of any resolution may be used. Different window sizes may also be used, and may produce significantly different results (see Riitters et al. 1997, 2002). As such, it is important that decision makers apply the model at a scale appropriate to the policy under development. Reporting units of any size may be used to summarize fragmentation, which allows for multi-scale assessments. For example, National Land Cover Data (NLCD; Vogelmann et al. 2001) could be used to examine fragmentation in the United States at 30-m resolution, using one or more window sizes. Summaries could be provided at the state, county, and watershed level, along with color composite and standard deviation maps.

Intuitively, forest fragmented by anthropogenic sources is at higher risk of further fragmentation or removal than forest fragmented by natural causes. Identifying only human-caused forest fragmentation may be a useful tool for policy and decision makers, allowing for improved risk assessments and better targeting of areas for protection or remediation. The method presented produces data that may be summarized and displayed in a myriad of ways, each of which may be useful to the decision process.

RESPONSES TO THIS ARTICLE

Responses to this article are invited. If accepted for publication, your response will be hyperlinked to the article. To submit a comment, follow [this link](#). To read comments already accepted, follow [this link](#).

Acknowledgments:

The United States Environmental Protection Agency (EPA), through its Office of Research and Development (ORD), partially funded and collaborated in the research described here under Interagency Agreement DW12939283-01-0 with the United States Department of Agriculture. It has been subjected to Agency review and approved for publication.

LITERATURE CITED

Bryant, D., D. Nielson, and L. Tangle. 1997. *The Last Frontier Forests: Ecosystems and Economies on the Edge*. World Resources Institute, Washington, D. C., USA.

Carvalho, K. S., and H. L. Vasconcelos. 1999. Forest fragmentation in central Amazonia and its effects on litter-dwelling ants. *Biological Conservation* **91**: 151–157.

Fearnside, P. M. 1996. Amazonian deforestation and global warming: carbon stocks in vegetation replacing Brazil's Amazon forest. *Forest Ecology and Management* **80**: 21–34.

Friedl, M. A., D. K. McIver, J. C. F. Hodges, X. Y. Zhang, D. Muchoney, A. H. Strahler, C. E. Woodcock, S. Gopal, A. Schneider, A. Cooper, A. Baccini, F. Gao, and C. Schaaf. 2002. Global land cover mapping from MODIS: algorithms and early results. *Remote Sensing of Environment* **83**: 288–303.

Gardner, R. H., B. T. Milne, M. G. Turner, and R. V. O'Neill. 1987. Neutral models for the analysis of broad-scale landscape pattern. *Landscape Ecology* **1**: 19–28.

Gascon, C., and T. E. Lovejoy. 1998. Ecological impacts of forest fragmentation in central Amazonia. *Zoology* **101**: 273–280.

Hargis, C. D., J. A. Bissonette, and D. L. Turner. 1999. The influence of forest fragmentation and landscape pattern on American martens. *The Journal of Applied Ecology* **36**: 157–172.

Holmgren, P. 2001. Forest area and area change. Pages 1–15 in A. Perlis, editor. *Global forest resources assessment 2000; Main report*. FAO Forestry Paper 140; FAO, Rome, Italy.

Jones, K. B., T. G. Wade, J. D. Wickham, K. H. Riitters, and C. M. Edmonds. 1999.

Characterizing Forest Fragmentation and Vulnerability Based on Patch Characteristics. USDA Forest Service Proceedings RMRS-P-12.

Jules, E. S., E. J. Frost, L. S. Mills, and D. A. Tallmon. 1999. Ecological consequences of forest fragmentation in the Klamath region. *Natural Areas Journal* **19**: 368–378.

Justice, C., D. Wilkie, Q. Zhang, J. Brunner, and C. Donoghue. 2001. Central African forests, carbon and climate change. *Climate Research* **17**: 229–246.

Kurki, S., A. Nikula, P. Helle, and H. Linden. 2000. Landscape fragmentation and forest composition effects on grouse breeding success in boreal forests. *Ecology* **81**:1985–1997.

Laurance, W. F. 2000. Mega-development trends in the Amazon: implications for global change. *Environmental Monitoring and Assessment* **61**: 113–122.

Laurance, W. F., H. L. Vasconcelos, and T. E. Lovejoy. 2000. Forest loss and fragmentation in the Amazon: implications for wildlife conservation. *Oryx* **34**: 39–45.

Loveland, T. R., and A. S. Belward. 1997. The IGBP-DIS global 1 km land cover data set, Discover first results. *International Journal of Remote Sensing* **18**: 3289–3295.

Loveland, T. R., B. C. Reed, J. F. Brown, D. O. Ohlen, Z. Zhu, L. Yang, and J. W. Merchant. 2000. Development of a global land cover characteristics database and IGBP DISCover from 1-km AVHRR data. *International Journal of Remote Sensing* **21**: 1303–1330.

Matthews, E. 2001. *Forest Briefing No. 1; Understanding the FRA 2000*. World Resources Institute, Washington, D. C., USA.

Matthews, E., R. Payne, M. Rohweder, and S. Murray. 2000. *Pilot Analysis of Global Ecosystems (PAGE): Forest Ecosystems*. World Resources Institute, Washington, D. C., USA.

Milne, B. T. 1992. Spatial aggregation and neutral models in fractal landscapes. *American Naturalist* **139**: 32–57.

Olson, D. M., E. Dinerstein, E. D. Wikramanayake, N. D. Burgess, G. V. N. Powell, E. C. Underwood, J. A. D'Amico, H. E. Strand, J. C. Morrison, C. J. Loucks, T. F. Allnutt, J. F. Lamoreux, T. H. Ricketts, I. Itoua, W. W. Wettengel, Y. Kura, P. Hedao, and K. Kassem. 2001. Terrestrial ecoregions of the world: a new map of life on Earth. *BioScience* **51**: 933–938.

Pahari, K., and S. Murai. 1999. Modelling for prediction of global deforestation based on the growth of human population. *Journal of Photogrammetry and Remote Sensing* **54**: 317–324.

Riitters, K. H., R. V. O'Neill, and K. B. Jones. 1997. Assessing habitat suitability at multiple scales: a landscape-level approach. *Biological Conservation* **81**: 191–202.

Riitters, K. H., and J. D. Wickham. 2003. How far to the nearest road? *Frontiers in Ecology and the Environment* **1**: 125–129.

Riitters, K., J. Wickham, R. O'Neill, B. Jones, and E. Smith. 2000. Global-scale patterns of forest fragmentation. *Conservation Ecology* **4**: 3. [Online] URL:

<http://www.consecol.org/vol4/iss2/art3>.

Riitters, K. H., J. D. Wickham, R. V. O'Neill, K. B. Jones, E. R. Smith, J. W. Coulston, T. G. Wade, and J. H. Smith. 2002. Fragmentation of continental United States forests. *Ecosystems* **5**: 815–822.

Scariot, A. 1999. Forest fragmentation effects on palm diversity in central Amazonia. *The Journal of Ecology* **87**: 66–76.

Semazzi, F. H. M., and S. Yi. 2001. A GCM study of climate change induced by deforestation in Africa. *Climate Research* **17**: 169–182.

Stauffer, D. 1985. *Introduction to Percolation Theory*. Taylor and Francis, Philadelphia, Pennsylvania, USA.

Virgos, E. 2001. Role of isolation and habitat quality in shaping species abundance: a test with badgers (*Meles meles* L.) in a gradient of forest fragmentation. *Journal of Biogeography* **28**: 381–389.

Vogelmann, J. E., S. M. Howard, L. Yang, C. R. Larson, B. K. Wylie, and N. van Driel. 2001. Completion of the 1990s National land cover data set for the conterminous United States from Landsat Thematic Mapper data and ancillary data sources. *Photogrammetric Engineering and Remote Sensing* **67**: 650–662.

Wickham, J. D., K. B. Jones, K. H. Riitters, T. G. Wade, and R. V. O'Neill. 1999. Transitions in forest fragmentation: implications for restoration opportunities at regional scales. *Landscape Ecology* **14**: 137–145.

Zhang, H., A. Henderson-Sellers, and K. McGuffie. 2001. The compounding effects of tropical deforestation and greenhouse warming on climate. *Climatic Change* **49**: 309–338.

Address of Correspondent:

Timothy G. Wade
U.S. Environmental Protection Agency,
E243-05,
Durham, North Carolina 27711 USA
Phone: (919) 541-4119
Fax: (919) 541-4329
wade.timothy@epa.gov

 [Return to Table of Contents for Volume 7, Issue 2](#)

[Main](#)

[Issues](#)

[How to Submit](#)

[Subscription Benefits](#)

Table 1. Original IGBP and re-classification used in the fragmentation analysis.

IGBP Classification	Reclassified to
1 Evergreen Needleleaf Forest	Forest
2 Evergreen Broadleaf Forest	Forest
3 Deciduous Needleleaf Forest	Forest
4 Deciduous Broadleaf Forest	Forest
5 Mixed Forest	Forest
6 Closed Shrublands	Other Natural
7 Open Shrublands	Other Natural
8 Woody Savannas	Forest
9 Savannas	Other Natural
10 Grasslands	Other Natural
11 Permanent Wetlands	Other Natural
12 Croplands	Anthropogenic
13 Urban and Built-Up	Anthropogenic
14 Cropland/Natural Vegetation Mosaic	Anthropogenic
15 Snow and Ice	Ignored
16 Barren or Sparsely Vegetated	Other Natural
17 Water Bodies	Ignored

Table 2. Percentage of biome area contained on each continent and percentage of global land surface area occupied by each biome.

Biome	Africa	Asia	Australia	Europe	N. America	S. America	Global
Tropical & Subtropical Moist Broadleaf Forest	17.66	21.89	13.79	0.00	3.16	43.50	14.98
Tropical & Subtropical Dry Broadleaf Forest	5.26	42.40	2.37	0.00	14.44	35.54	2.74
Tropical & Subtropical Coniferous Forest	0.00	12.35	1.41	0.00	86.24	0.00	0.53
Temperate Broadleaf & Mixed Forest	0.01	27.66	5.73	41.41	22.25	2.95	9.69
Temperate Conifer For.	0.57	31.39	0.00	11.72	56.32	0.00	3.09
Boreal Forests/Taiga	0.00	50.44	0.00	15.73	33.83	0.00	11.43
Mediterranean	26.54	0.00	25.07	40.02	3.75	4.63	2.43
Mangroves	23.16	24.18	18.16	0.00	17.03	17.47	0.23

Table 3. Percent of re-classified land cover by World Wildlife Fund biome and continent. Bold indicates biomes that occupy more than 10% of the continent land area. For example, 7.7% of the land area in Africa is re-classified forest in the Tropical and Subtropical Moist Broadleaf Forest biome. Columns do not sum to 100 because only forest biomes are included.

Biome	Africa			Asia			Australia			Europe			N. America			S. America		
	F	N	A	F	N	A	F	N	A	F	N	A	F	N	A	F	N	A
Tropical & Subtropical Moist Broadleaf Forest	7.7	1.7	2.2	8.2	1.0	9.9	15.1	2.1	7.7	0	0	0	1.8	0.2	1.0	38.4	3.4	6.4
Tropical & Subtropical Dry Broadleaf Forest	0.1	0.4	0.1	1.2	0.1	5.4	0.4	<0.1	0.4	0	0	0	1.5	0.2	0.9	4.1	1.5	1.8
Tropical & Subtropical Coniferous Forest	0	0	0	0.1	0.1	0.2	<0.1	<0.1	0.1	0	0	0	2.0	0.3	0.6	0	0	0
Temperate Broadleaf & Mixed Forest	<0.1	<0.1	<0.1	4.1	1.8	7.2	4.0	1.4	1.3	6.1	3.1	24.5	8.5	<0.1	4.9	1.3	0.5	0.1
Temperate Conifer For.	<0.1	<0.1	<0.1	1.3	2.0	0.5	0	0	0	1.1	0.7	1.2	8.2	1.3	1.4	0	0	0
Boreal Forests/Taiga	0	0	0	0.4	0.1	<0.1	0	0	0	11.7	0.8	1.9	12.8	10.2	0.2	0	0	0
Mediterranean	0.2	2.4	0.3	0	0	0	1.4	3.4	2.7	1.2	1.6	5.4	0.3	0.2	<0.1	0.1	0.5	0.2
Mangroves	0.1	0.1	0.1	<0.1	0.1	0.2	0.3	<0.1	0.1	0	0	0	0.1	<0.1	0.1	0.2	<0.1	0.1

Table 4. Percentage of connected (C; $P_{ff} \geq 60\%$) and interior (I; $P_{ff} = 100\%$) forest pixels by continent and biome. For any combination of continent and biome, the sum of percentages may exceed 100% because connected forest includes interior forest by definition, and the sum may be less than 100% as not all forest is connected or interior.

Biome	Africa		Asia		Australia		Europe		N. America		S. America	
	C	I	C	I	C	I	C	I	C	I	C	I
Tropical & Subtropical Moist Broadleaf Forest	69.58	38.15	43.64	16.11	61.27	20.99	NA	NA	59.57	12.65	81.56	49.12
Tropical & Subtropical Dry Broadleaf Forest	28.15	2.01	18.58	2.47	46.89	3.77	NA	NA	60.26	19.83	60.02	23.70
Tropical & Subtropical Coniferous Forest	NA	NA	30.83	7.11	25.49	13.02	NA	NA	73.48	23.03	NA	NA
Temperate Broadleaf & Mixed Forest	35.65	0.00	38.08	12.32	65.29	27.53	17.02	2.02	64.77	27.06	74.98	26.79
Temperate Conifer For.	40.34	1.31	57.84	24.79	NA	NA	37.45	2.09	80.03	32.87	NA	NA
Boreal Forests/Taiga	NA	NA	85.95	48.52	NA	NA	83.03	43.26	74.75	41.77	NA	NA
Mediterranean	16.66	0.37	NA	NA	26.83	3.30	13.99	0.38	65.75	18.03	18.00	7.70
Mangroves	31.94	1.08	17.38	0.57	70.40	30.38	NA	NA	32.77	2.20	56.10	9.83

Table 5. Average percent P_{fa} and P_{fn} by World Wildlife Fund biome and continent. Higher values indicate more fragmentation, and the ratio of P_{fa} to P_{fn} indicates the relative importance of human-caused fragmentation compared with natural fragmentation.

Biome	Africa		Asia		Australia		Europe		N. America		S. America		Global	
	Pfa	Pfn	Pfa	Pfn	Pfa	Pfn	Pfa	Pfn	Pfa	Pfn	Pfa	Pfn	Pfa	Pfn
Tropical & Subtropical Moist Broadleaf Forest	18.33	8.63	48.40	3.69	29.85	6.34	NA	NA	30.82	6.40	13.43	4.21	24.87	5.22
Tropical & Subtropical Dry Broadleaf Forest	24.21	35.69	75.72	0.98	44.35	1.59	NA	NA	31.14	5.11	24.74	11.35	48.80	6.48
Tropical & Subtropical Coniferous Forest	NA	NA	44.53	13.68	66.77	0.25	NA	NA	17.93	8.41	NA	NA	21.71	8.90
Temperate Broadleaf & Mixed Forest	19.42	24.59	49.91	8.51	17.80	14.97	73.67	1.46	33.74	0.23	7.01	17.96	52.78	4.36
Temperate Conifer For.	30.82	20.50	13.33	24.01	NA	NA	45.05	9.64	11.61	9.37	NA	NA	15.88	13.64
Boreal Forests/Taiga	NA	NA	2.97	11.54	NA	NA	12.90	4.36	1.25	21.65	NA	NA	4.18	13.09
Mediterranean	35.45	36.03	NA	NA	45.62	22.10	68.83	9.59	6.34	26.70	65.96	8.31	55.38	16.94
Mangroves	26.24	29.42	73.95	4.15	22.42	4.79	NA	NA	41.10	13.65	30.01	7.88	39.30	12.51

Table 6. Average percent P_{fa} and P_{fn} by WWF ecoregion for the tropical and subtropical moist broadleaf forest biome in South America. Higher values indicate more fragmentation.

Ecoregion	P_{fa}	P_{fn}
Araucaria moist forests	34.09	30.08
Atlantic Coast restingas	40.87	27.60
Bahia coastal forests	44.75	28.16
Bahia interior forests	37.58	27.44
Bolivian Yungas	12.40	16.75
Caatinga Enclaves moist forests	60.74	33.00
Caqueta moist forests	4.95	9.70
Catatumbo moist forests	25.40	27.85
Cauca Valley montane forests	40.08	23.88
Chocó-Darién moist forests	31.01	24.52
Cordillera La Costa montane forests	16.76	20.27
Cordillera Oriental montane forests	20.36	21.71
Eastern Cordillera real montane forests	37.06	28.99
Eastern Panamanian montane forests	33.32	22.81
Guayanan Highlands moist forests	3.53	9.76
Guianan moist forests	5.49	12.73
Gurupa varzeá	12.07	15.74
Iquitos varzeá	4.63	9.38
Japurá-Solimoes-Negro moist forests	3.33	7.37
Juruá-Purus moist forests	2.42	5.42
Madeira-Tapajós moist forests	4.79	11.02
Magdalena Valley montane forests	31.85	26.99
Magdalena-Urabá moist forests	42.70	37.54
Marajó Varzeá forests	14.20	15.09
Maranhao Babat u forests	41.16	35.78
Mato Grosso seasonal forests	8.49	18.00
Monte Alegre varzeá	8.10	12.41
Napo moist forests	5.18	10.56
Negro-Branco moist forests	3.76	8.83
Northeastern Brazil restingas	71.63	24.48
Northwestern Andean montane forests	36.37	29.24
Orinoco Delta swamp forests	16.17	19.52
Guianan Freshwater swamp forests	21.44	19.79
Alta Paraná Atlantic forests	44.02	35.50
Pernambuco coastal forests	85.57	18.38

Pernambuco interior forests	86.75	19.60
Peruvian Yungas	22.10	23.23
Purus varzeá	3.43	6.62
Purus-Madeira moist forests	3.82	7.87
Rio Negro campinarana	6.47	11.82
Santa Marta montane forests	44.00	30.59
Serra do Mar coastal forests	38.40	29.25
Solimoes-Japurá moist forest	2.84	5.69
Southern Andean Yungas	17.58	24.99
Southwest Amazon moist forests	2.02	6.57
Tapajós-Xingu moist forests	2.54	6.13
Tepuis	13.67	17.55
Tocantins/Pindare moist forests	25.47	25.68
Trinidad and Tobago moist forests	21.28	22.84
Uatuma-Trombetas moist forests	3.75	8.55
Ucayali moist forests	6.76	13.04
Venezuelan Andes montane forests	20.30	21.62
Western Ecuador moist forests	49.59	27.87
Xingu-Tocantins-Araguaia moist forests	6.42	11.42

Fig. 1. World Wildlife Fund biomes. After Olsen et al. (2001). Click on image for larger version.

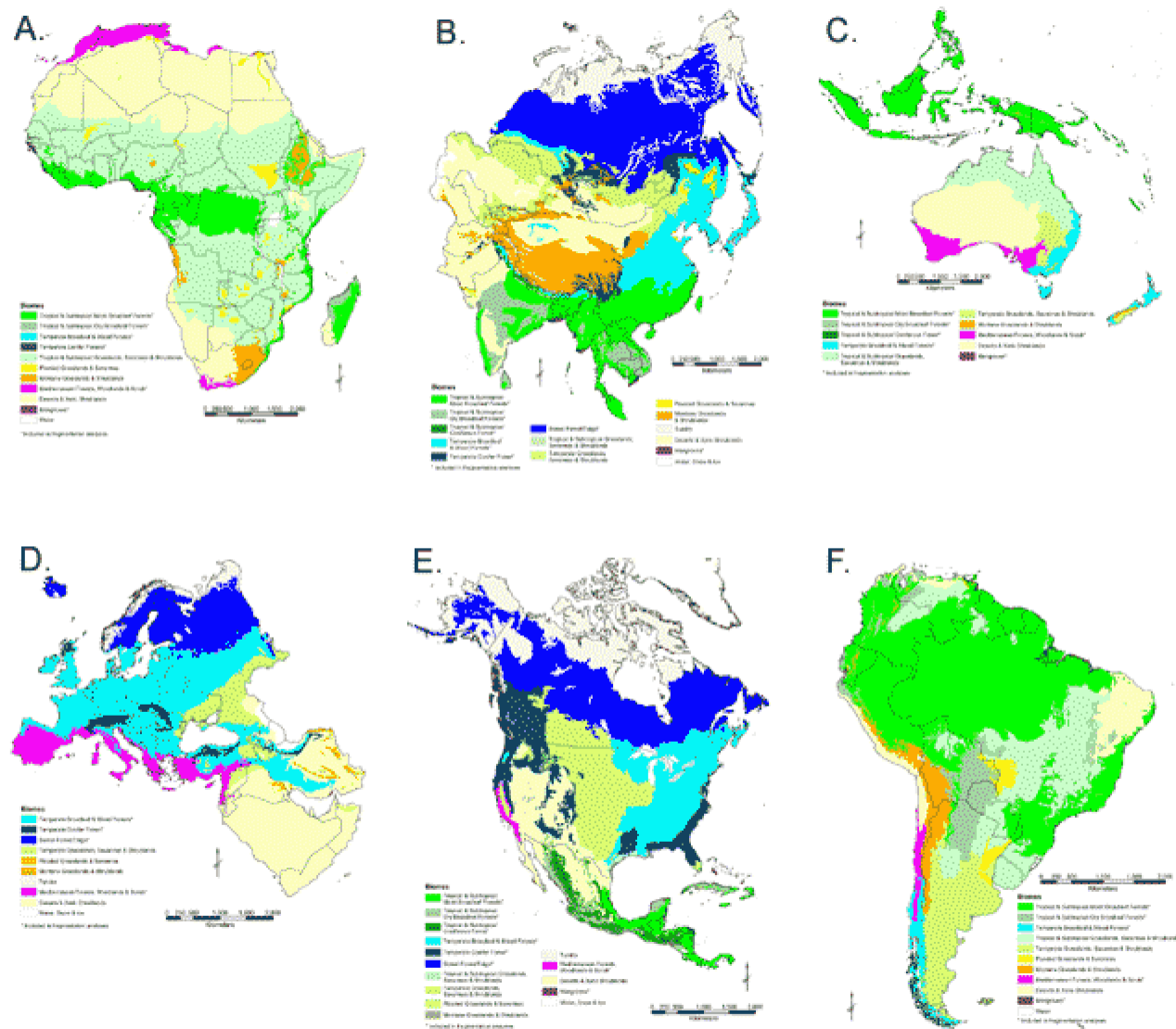



Fig. 2. Example showing the calculation of P_{fa} , P_{fn} , and P_{ff} in a 3×3 pixel analysis window containing three types of land cover. An “edge” is the imaginary line that separates any two adjacent pixels. The analysis presented used 9×9 pixel analysis windows. See text for additional explanation.

A	A	N	A = Anthropogenic land-use, N = Non-forest natural land-cover and F = Forest	
N	F	F	Total F-A edges = 1	$P_{fa} = 1 / 8$
			Total F-N edges = 3	$P_{fn} = 3 / 8$
			Total F-F edges = 4	$P_{ff} = 4 / 8$
N	F	F	Total F-any edges = 8	

Fig. 3. Scatter plot of the proportion of forest (P_f) vs. anthropogenic fragmentation (P_{fa}) for each combination of continent and biome. The horizontal lines drawn at $P_f = 40$ and 60 represent possible thresholds of connectivity (see text). For a given value of P_f , the relative value of P_{fa} may help identify biomes and continents where anthropogenic fragmentation is more or less of an issue.



Fig. 4. Color composite showing the components of fragmentation. Pixels are individually rendered according to their measured values for P_{ff} , P_{fa} , and P_{fn} (see text for explanation). Black represents continuous areas of non-forest natural land cover, and white areas were not included in the study. Click on an image for a quick loading, larger version or select the appropriate pdf link for a high resolution, larger version.

 Note: PDF files may not display correctly in some web browsers. We recommend downloading PDF files and viewing from your desktop. To do this, hold the shift key down when clicking the link.

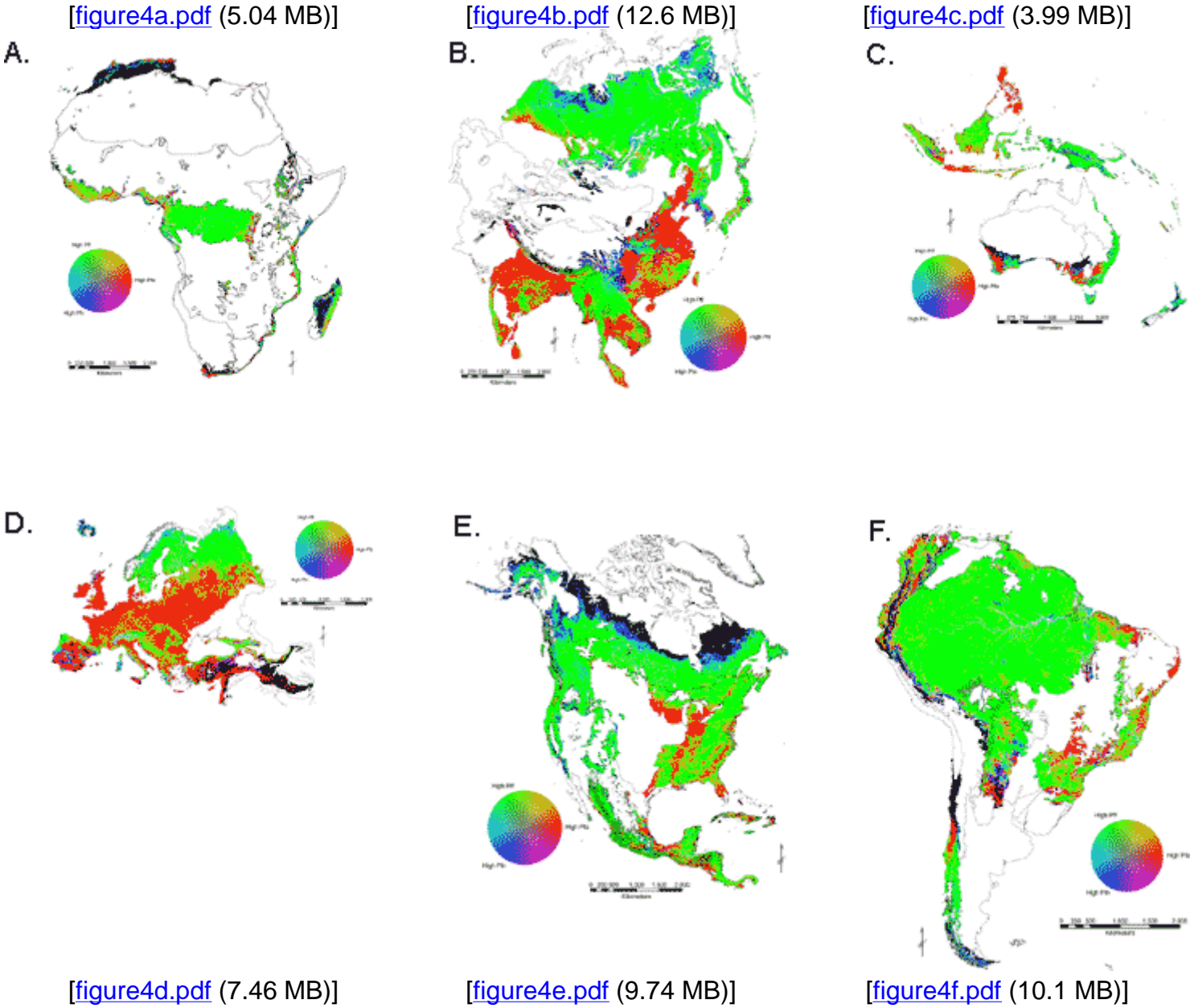
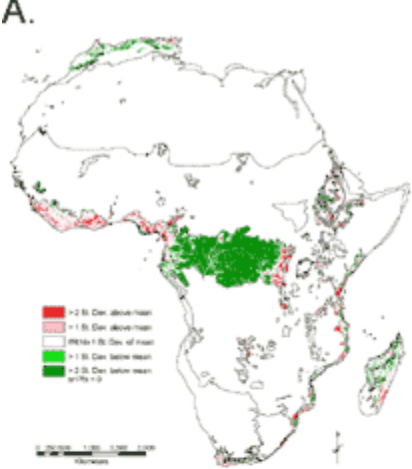


Fig. 5. The locations of extreme values of the P_{fa} statistic. Click on an image for a quick loading, larger version or select the appropriate pdf link for a high resolution, larger version.



Note: PDF files may not display correctly in some web browsers. We recommend downloading PDF files and viewing from your desktop. To do this, hold the shift key down when clicking the link.

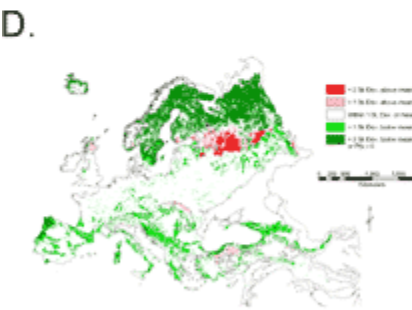
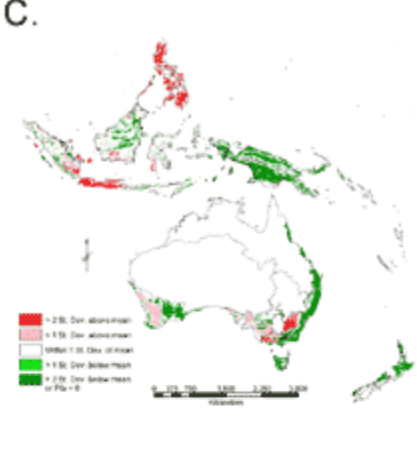
[\[figure5a.pdf \(866 KB\)\]](#)



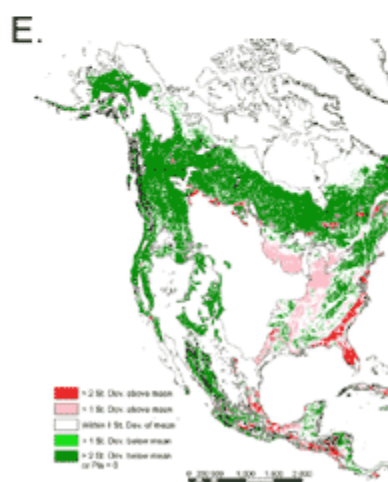
[\[figure5b.pdf \(1.83 MB\)\]](#)



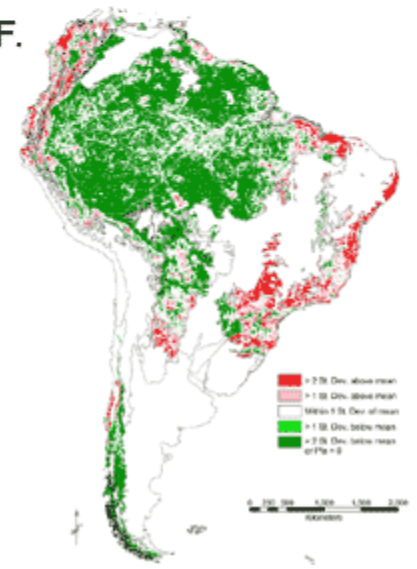
[\[figure5c.pdf \(670 KB\)\]](#)



[\[figure5d.pdf \(1.05 MB\)\]](#)



[\[figure5e.pdf \(2.45 MB\)\]](#)



[\[figure5f.pdf \(1.63 MB\)\]](#)